Combination of Lagrangian Discrete Phase Model and sediment physico-chemical characteristics for the prediction of the distribution of trace metal contamination in a stormwater detention basin

Xiaoxiao Zhu, Vincent Chatain, Mathieu Gautier, Denise Blanc-Biscarat, Cécile Delolme, Nathalie Dumont, Jean-Baptiste Aubin, Gislain Lipeme Kouyi

Combination of Lagrangian Discrete Phase Model and sediment physico-chemical characteristics for the prediction of the distribution of trace metal contamination in a stormwater detention basin

Xiaoxiao Zhu[1,*], Vincent Chatain[1], Mathieu Gautier[1], Denise Blanc-Biscarat[1], Cécile Delolme[1], Nathalie Dumont[1], Jean-Baptiste Aubin[1], Gislain Lipeme Kouyi[1]

[1]University of Lyon, INSA Lyon, DEEP, F-69621 Villeurbanne cedex, France

*Corresponding author: Xiaoxiao Zhu (xiaoxiao.zhu@insa-lyon.fr)

Abstract

Elevated trace metal concentrations in sediments poses a major problem for the management of stormwater detention basins. These basins provide a nature-based solution to remove particulate pollutants through settling, but the resuspension of these contaminated deposits may impact the quality of both surface and groundwater. A better understanding of trace metal distribution will help to improve basin design and sediment management. This study aims to predict the distribution of trace metal contamination in a stormwater detention basin through (i) investigation of the correlation between metal content in sediments and their settling velocity, and (ii) the coupling of such correlation with a Lagrangian Discrete Phase Model (LDPM). The correlation between Fe, Cr, Cu, Ni, Pb contents and the settling velocity is firstly investigated, based on the sediments collected from 6 sites (inlet and 5 traps at the bottom of a detention basin situated in Chassieu, France) during 5 campaigns in 2017. Results show that Fe is strongly correlated to settling velocity and can be considered as a good indicator of trace metal contents. The derived correlation is then combined with a LDPM for the prediction of trace metal distribution, producing results consistent with *in situ*

measurements. The proposed methodology can be applied for other stormwater basins (dry or wet). As described in this article, the interactions between hydrodynamics and sediment physico-chemical characteristics is crucial for the design and management of stormwater detention basins, allowing managers to target the highest contaminated sediments.

Key words: Hydrodynamics, Metal contamination, Sediment, Settling velocity, Stormwater treatment

1. Introduction

Stormwater detention basins, among the many stormwater control measures (SCMs), are used to intercept and trap sediments by sedimentation (e.g. Marsalek and Marsalek 1997; Maniquiz-Redillas et al., 2014). They are widely used in most developed countries, such as France, Canada, US and other European countries (Urbonas, 1994). Since most of the pollutants, such as trace metals, polycyclic aromatic hydrocarbons (PAHs) and some pathogenic bacteria, are transported in a predominantly particulate form in urban stormwater (e.g. Barbosa et al., 2012; Gasperi et al., 2014; Zgheib et al., 2012), stormwater detention basins play an important role in the decontamination of stormwater by means of settling processes. A better understanding of key mechanisms in these basins is important to improve hydraulic and pollutant removal performance. Sediment movement in detention basins or reservoirs depend on their characteristics, e.g. size, shape, cohesive aspect, density, and settling velocity (Loch, 2011). It also depends on the residence time, which in return is controlled by the basin's geometry and flow patterns (Verstraeten and Poesen, 2000; Zhang, 2009; Akan, 2010). While the interactions between hydrodynamics and physico-chemical characteristics are of importance, they have not commonly been considered during the basin design phase, which to date has been primarily focused on hydraulic performance (e.g. Persson, 2000). In addition, the accumulated contaminated

43 deposits can be resuspended by incoming stormwater, subsequently being transported to the
44 downstream aquatic environment. Sediment aerosolization could also pose a microbiological risk for
45 humans through inhalation of aerosols during maintenance (Bernardin-Souibgui et al., 2018). Hence,
46 appropriate management of accumulated contaminated sediments is crucial. Sustainable management
47 of contaminated sediments is challenging, due to (i) expensive transportation, treatment and recycling
48 fees, and (ii) limited reliable and suitable treatment and recycling options (e.g. Petavy et al., 2009). It
49 is therefore essential to determine the distribution of contamination in stormwater detention basins
50 and target the priority zones for treatment and intervention.

51 A thorough geochemical characterization of settled sediments can be used to determine the
52 contamination distribution in stormwater detention basins. (Jang et al., 2010; Tedoldi et al., 2017).
53 However, a large number of samples are needed, and their collection and characterization are
54 expensive and time-consuming. Numerical models, on the other hand, are an effective and low-cost
55 approach to predict the distribution of contamination. A chemical model was proposed by Vezzaro et
56 al. (2010) to simulate the removal of micropollutants in such basins based on relevant removal
57 processes, such as settling, volatilization, sorption, biodegradation and abiotic degradation. This
58 model, however, fails under complex hydrodynamic conditions in basins (Sebastian et al., 2014c) as
59 the interactions between hydrodynamics and physico-chemical characteristics are ignored. The
60 combination of Lagrangian Discrete Phase Model (LDPM) and the correlation between physical and
61 chemical characteristics can be an appropriate alternative. Indeed, the simulation of particle transport
62 provides a quick, convenient and low-cost way to characterise particle movement and predict
63 preferential deposition zones of the particles and their associated pollutants. Such an approach permits
64 alternative basin geometries to be compared, facilitating the design process. For example, a LDPM

implemented in computational fluid dynamics (CFD) package allows particle transport mechanisms in stormwater detention basins to be simulated, with particle physical characteristics used as model inputs (Adamsson et al., 2003; Yan et al., 2014). Finally, the transport mechanisms of pollutants can be simulated by implementing the correlation between particle physical and chemical characteristics using outputs of LDPM simulations or other solid transport model results.

Trace metals are considered as priority stormwater chemical pollutants related to urban activities. The decision No. 2455/2001/EC issued by the European Parliament and Council listed 33 priority substances, including Ni, Pb and their compounds. Zgheib et al. (2008) extended the list to 88 individual substances, including Cr and Cu. Iron, as a major earth element, plays a key role in the geochemistry of soils and sediments and is of great importance to many metals cycling processes (Taylor and Kauhauser, 2011). Iron oxides are also important for the sorption of trace metals (Bradl, 2004; Whitaker and Duckworth, 2018). As far as physical characteristics are concerned, settling velocity is an integrated property of particulate pollutants, as it is related to multiple characteristics such as diameter, density, shape and surface roughness (Loch, 2001). Several investigations are reported in the literature regarding both trace metal contents (Becouze-Lareure et al., 2019; Sébastian et al., 2014a) and particles' settling velocities in stormwater detention basins (Torres et al., 2007; Yan et al., 2014). However, to the best of our knowledge, little is known concerning the relationship between metal contents, particularly Fe, and settling velocity in urban stormwater detention components. Bentzen and Larsen (2009) investigated such relationship in a wet detention pond of road runoff, where high Cd, Cr, Zn and Ni contents were found associated with low settling velocities while the tendency for Cu and Pb was unclear. However, the conclusions were empirically drawn without quantitative analyses. Torres et al. (2007) found a significant correlation among median

87 settling velocity (V50) and contents of Cd, Cu, Pb and Zn in a stormwater detention basin, but metal
88 contents with respect to different fractions of settling velocities were not considered. Overall, a
89 thorough analysis of the correlation between metal contents and settling velocity and the importance
90 of Fe have not been considered in previous work.

91 The objective of this article is to predict the spatial distribution of trace metal contamination through
92 (i) the investigation of the correlation between metal contents (major element: Fe and some trace
93 metals: Cr, Cu, Ni and Pb) in trapped sediments and their settling velocity in a stormwater detention
94 basin, and (ii) the implementation of such correlations in a LDPM, taking into considerations the
95 interactions between hydrodynamics and particle physico-chemical characteristics.

96 ## 2. Methods and materials

97 ### *2.1. Experimental site and sampling locations*

98 Our work was conducted in the Django Reinhart stormwater detention basin (DRB), which remains
99 dry during dry weather. The DRB is a part of the broader facilities investigated within the framework
100 of the Field Observatory for Urban Water Management (or OTHU in French,
101 http://www.graie.org/othu/ - see also Zhu and Lipeme Kouyi, 2019). Fig. 1a provides a panoramic
102 photograph of DRB, while its characteristics are presented in Table 1.

103 **Fig. 1. (a) Panorama of DRB, (b) hydrocyclone trapping system at the inlet 1 of DRB, (c) sketch**
104 **of DRB and sampling points, (d) honeycomb-like sampling traps**

Table 1. Characteristics of DRB

Sediments were collected from six sampling sites, five of which are situated at the base of DRB (P01, P02, P04, P07, P12bis, illustrated in Fig. 1c). The sampling sites were selected according to sediment accumulation zones and previous studies (Sébastian et al., 2014b; Torres et al., 2007; Yan et al., 2014). Stormwater enters from the inlet situated at the lower-right side, and creates a counterclockwise swirl at the centre of the basin (shown in yellow in Fig. 2). There are then several flow paths within the basin (in orange, green, red and magenta in Fig. 2). Sampling points P01 and P02 are prone to trap medium-sized particles (median size D50 of 40 - 200 µm), given their locations near the basin inlet and at the middle of a flow path, respectively. Points P04 and P07 are situated at the end of the flow path where fine particulate particles (median size D50 of 25 - 70 µm) are expected to be trapped. Indeed, Jacopin et al. (1999) revealed the same trend i.e. the finest particles are found in the furthest part from the inlet of detention/retention basin. Point P12bis is a specific sampling site near a small tank designed to trap hydrocarbons, where medium and coarse particles are usually found (median size D50 of 200 µm). For each point, 3 honeycomb-like traps (Fig. 1d) were placed at the bottom. A hydrocyclone system was designed as a sampling device and installed at the inlet (illustrated in Fig. 1b) in order to intercept particulate pollutants from the inlet of basin (Zhu et al., 2016).

Fig. 2. Streamline of the liquid phase flow obtained by computational fluid dynamics simulations (Q = 0.35 m^3/s, mean flow rate) and characteristics of sediments: (a) locations of settled particles of different sizes shown in different colors: red circles for coarse particles (D50 > 500 µm), yellow for medium ones (D50 average 40 µm), and green for fine ones (D50 average 25 µm). (b) locations of different sampling sites (P01, P02, P04, P07, P12bis) at the base of DRB.

2.2. *Presentation of campaigns*

Five campaigns were conducted during rain events in 2017 (from spring to winter). Nineteen sediment samples from 6 sites were collected and characterized (summarized in Fig. 3). The main characteristics of the sampled rain events and their corresponding hydraulic parameters in the detention basin are presented in Table 2.

Fig. 3. Campaign timeline and sampling points for each campaign

Table 2. Characteristics of the sampled rain events and corresponding hydraulic parameters in DRB

2.3. *Methodology to predict distribution of trace metal contamination*

2.3.1. *Physical and chemical characterizations and determination of their correlation*

In this study, particle-size distribution, settling velocity distribution and metal contents in sediments were analysed, according to the standards and protocols listed in Table 3.

Table 3. Standard and protocols for physical and chemical analyses

The VICAS protocol (a French acronym for Effluent Settling Velocity, Chebbo et al., 2009) is applied to measure settling velocity distribution. It is based on the principle of homogeneous suspension, where the solids are uniformly distributed over the entire sedimentation height. The measurement is realised with a plexiglas sedimentation column in the laboratory. The settled solids at a set of 10 predefined time points (t = 1, 2, 4, 8, 16, 32min, 1, 2, 4, > 24h) are manually collected at the bottom of the sedimentation column in aluminium receptacles. The evolution of accumulated mass of settled particles over time is then determined by measuring the mass in each receptacle, which yields the

146 settling velocity distribution curve. Meanwhile, the average settling velocity in each receptacle
147 defined in Eq. 1 is used to investigate the correlation between metals contents and settling velocity:

$$Vs = \frac{H}{t} \quad \text{Eq. 1}$$

148 where Vs denotes particle settling velocity (mm/s), H is water height in the sedimentation column
149 (mm) and t is the time point (s) when the receptacle with collected particles is removed.

150 Metals contents in particles are then analysed with ICP-OES (inductively coupled plasma optical
151 emission spectrometry) method. The total suspended solids (TSS) are filtered through glass fibre
152 filters (0.45 µm) and dried at 105 °C (French standard NF EN 872, 2005). Mineralization is then
153 applied in order to extract soluble elements from particles with aqua regia (NF EN 16174, 2012). The
154 obtained solution is finally diluted to 50 ml, filtered at 0.45 µm and analysed with ICP-OES
155 equipment. For each element, the limit of detection (LOD) is calculated from the calibration. The limit
156 of quantification (LOQ) is considered to be 3.3 times of LOD. In our study, as a precaution, only the
157 values larger than 3 times of LOQ were considered as quantifiable.

158 Fig. 4 shows the methodology of physical and chemical characterizations. Two groups of data
159 (physical and chemical characteristics) were gathered from the collected samples, in order to,
160 respectively, (i) obtain overall physical and chemical characterization of samples and associated
161 global relationships and (ii) reveal in particular the correlation between metals contents and settling
162 velocity, as well as its significance. The first group (Data of group I) consists of particle-size
163 distribution, settling velocity distribution and metal contents (Fe, Cr, Cu, Ni and Pb) of 19
164 sub-samples (deriving from the 19 original samples). The second group (Data of group II) consists of
165 settling velocities and metals contents (Fe, Cr, Cu, Ni and Pb) of 190 sub-samples under the VICAS

protocol. For each of the 19 samples, 10 sub-samples, i.e. receptacles of particles removed from the bottom of experimental column at all the 10 predefined time points t, have different settling velocities (described by Eq. 1). For each receptacle, metal contents in collected sediments are measured.

Fig. 4. Methodology of physical and chemical characterizations

Several statistics have been computed, including: (i) principal components of physical and chemical characteristics of group I via PCA (Principal Component Analysis), (ii) correlation between metals contents and settling velocity based on the data of group II and test of significance, and (iii) correlation matrix for all metals accounting for data of group II. In this study, Spearman's rank correlation coefficient is applied as the settling velocities are not normally distributed according to the Shapiro-Wilk test (Shapiro and Wilk, 1965) and a monotonic relationship is observed between metal contents and settling velocity. Significance tests of correlation coefficient are also carried out by comparing p-value to a significance threshold (denoted as α, equal to 0.05 by default). Bonferroni correction (Dunnett, 1955) is applied to reduce false positive (Type I) errors when multi-comparisons are applied. In order to set FWER (Family-wise error rate) lower than α, it rejects the null hypothesis with $p - value$ as follows:

$$p - value \leq \frac{\alpha}{m} \quad \text{Eq. 2}$$

where m is the total number of null hypotheses.

2.3.2. Strategy to combine derived correlations with LDPM

LDPM was employed to simulate sediment transport in DRB (Yan et al., 2014). The flow was firstly simulated in steady state condition and then used as a base for further sediment transport modelling with a Lagrangian approach. The model was evaluated and had a good fit with both *in situ* free surface velocity field measurement results (Zhu et al., 2019) and measured accumulated sediment distribution at the bottom of DRB (Yan et al., 2014). LDPM approach allows the computation of particles trajectories. The interaction between sediments and the bottom wall was modelled by an original boundary condition based on turbulent kinetic energy threshold (Yan et al., 2014). During LDPM simulations, the location in the DRB as well as the physical characteristics (settling velocity, particle size and density) of sediments was recorded. The focus was placed on the settled particles as they represent accumulated sediments or deposits in the DRB. The metals contents distributions were then computed by combining the correlation between metals contents and settling velocity with recorded simulated data deriving from LDPM approach.

3. Results

3.1. Physical and chemical characteristics from data of group I

Physical and chemical characteristics are illustrated in Table 4. In general, settling velocity varies with campaign and site, consistent with previous work (e.g. Torres et al., 2007). The samples collected from the inlet show the most significant temporal variability, with median settling velocity ranging from 1.9 to 11.6 m/h. Trapped particles from P01 have higher settling velocities than those from the other sampling sites at the base of DRB. Indeed, the location P01 is near the inlet where heavy particles settle rapidly, as demonstrated e.g. by Jacopin et al. (1999).

As illustrated in Table 4, Fe contents are at least 36 times higher than Cu contents and up to 200 times higher than the other trace metals contents (Cr, Ni and Pb). As for trace metals, Cu, Ni and Pb

contents exceed the target values of Dutch standards (DTIV, 2000). Cu contents, as well as Pb contents in some cases, surpass even the intervention threshold. It is noticed that Fe contents at the inlet are lower (average 16.9 g/kg DM) than those observed in the basin (average 20.7-23.9 g/kg DM), in opposition to trace metals. Besides, samples collected from the inlet show a significant temporal variability, with a coefficient of variation of approximately 50%.

Fig. 5 shows PCA results of all physical and chemical variables (particle size, settling velocity and metals contents). Principal component 1 (PC1) explains 48.9% of variance, while PC2 explains 22.9%. Overall, settling velocities are highly related among themselves (V20, V50 and V80). The same conclusion can be drawn for particle sizes (D10, D50 and D90). The relationship among different metals, as well as that between metal contents and settling velocities or sizes, is unclear. Temporal variability is observed as expected. Event C3 is a storm of high rain intensity and maximum inlet flow rate but low total depth and rain duration. Event C4 is a rain event of the highest total depth and maximum water level in DRB. This may lead to strong variation of spatial distribution of sediments due to shear stress (Adamsson et al., 2003) or turbulence in DRB (Sechet and Le Guennec, 1999). Significant temporal variability is particularly observed for particles intercepted by the hydrocyclone device at the inlet of the basin. Among particles trapped at the base of DRB, those at P02 seem to be different from particles observed at other sites, characterized by their low settling velocities and high metal contents, regardless of the campaign. In fact, particles with high settling velocities tend to settle near the inlet (P01), while P02 is in the main recirculation zone with long residence time which enables particles to settle progressively (Zhu and Lipeme Kouyi, 2019).

Table 4. Physical and chemical characteristics of trapped sediments

Fig. 5. Principal component analysis (PCA) of physical and chemical characteristics based on the data of group I

3.2. Correlation between metals contents and settling velocity, and correlation matrix for different metals based on data of group II

All the results from different campaigns (C1-C5) and sampling sites (inlet, P01, P02, P04, P07 and P12bis) are presented in Fig. 6 (a-e) to analyse the correlation between metals contents and settling velocity. Fig. 6 (f-j) are boxplots of different metals contents with respect to settling velocity. In general, results show that contents of the metals in settled sediments are relatively stable, with values varying within ranges of 15-35 g/kg, 20-120, 200-650, 20-150 and 50-250 mg/kg DM for Fe, Cr, Cu, Ni and Pb, respectively, except for a few outliers. [Fe] and [Pb] have significant correlations with $\log(Vs)$ after Bonferroni correction, especially in the case of [Fe], with a correlation coefficient equal to -0.52. Higher [Fe] and [Pb] are related to lower settling velocity. The best fit of their correlations are illustrated in Fig. 6a and Fig. 6e and can be defined by the equation shown at the upper-right side. [Cu] tends to decrease slightly with the increasing of Vs, in opposite to [Cr]. Indeed, previous works suggest that Fe contents are relatively stable, while Cu can be variable in stormwater environment given its affinity with organic matter (Camponelli et al., 2010). No obvious correlation is observed between [Ni] and Vs. The dispersion around the regression line (marked as red dashed lines for 95% confidence interval) is related to spatio-temporal variabilities of metal contents and settling velocity distributions, physico-chemical processes and characteristics, as well as uncertainties in sampling and analytical measurements (Torres and Bertrand-Krajewski., 2008; Sébastian et al., 2015). The physico-chemical analyses conducted by Becouze-Lareure et al. (2018) show a high organic matter content for the trapped sediments in DRB. This may lead to changes in the physico-chemical

conditions in the sediments, which could affect the solubility and availability of certain trace metals. These different processes and assumptions have already been observed in various investigations focusing on urban sediments, such as those from rivers (Chapman et al., 1998) and from reservoirs (Frémion et al., 2016; Frémion et al., 2017). Torres et al. (2007) also showed the spatial and temporal variability of settling velocity of DRB sediments.

Fig. 6. (a-e) Correlation between metals contents [M] in g/kg DM and settling velocity (Vs) in mm/s based on data of group II; (f-j) Boxplot of different [M] with respect to each Vs.

The correlation matrix among different metals contents is also calculated (shown in Fig. 7). Results show that almost all the studied metals have significant correlations with each other except for Cr versus Fe and Ni versus Pb. Fe and Pb are the most related metals, with a correlation coefficient of 0.61.

Fig. 7. Correlation matrix of different trace metals contents in trapped particles: the distribution of each variable is listed on the diagonal. The bivariate scatter plots with their linear fits are displayed below the diagonal. The upper triangle contains the correlation coefficients and their significance levels. Each significance level is associated to a symbol: p-values of 0.001, 0.01, 0.05, 0.1 correspond to symbols of *, **, * and ▪, respectively.**

3.3. Prediction of trace metals contamination distribution

Given the significant correlations of Fe and Pb contents with settling velocity, the derived correlations (equation in Fig. 6) were applied on LDPM outputs to simulate the spatial distribution of Fe and Pb contents in DRB. Fig. 8 illustrates the comparison of the measured and simulated distribution of Fe and Pb contents at the base of DRB. The simulated [Fe] at P01, P02, P04 and P07 are consistent with

the measurements obtained from group I, where P07 and P02 have the highest [Fe] in sediments. P07 shows a significant variation in [Fe]. Indeed, P07 is situated at the end of pathway, where sediments tend to be resuspend, as previous work has suggested (Zhu et al., 2017). In addition, P07 is near an orifice, which may lead to maximum flow shear and velocities around this site and through the orifice, increasing variability due to dispersion of sediments (e.g. interaction between burst and bedload transport, see e.g. Sechet and Le Guennec, 1999). Simulated [Pb] in DRB is around 129 mg/kg DM, which is not consistent with the measurements due to temporal variability. However, the results are consistent when comparing the simulated Fe contents distribution with the measured Pb contents at different sampling points. Indeed, significant positive correlation between Fe and Pb is revealed in Fig. 7. Hence, it is interesting to use Fe as an indicator to predict other metals contents distribution. Uncertainties with 95% confidence interval of ± 8.8 g/kg and ± 69.4 mg/kg for Fe and Pb, respectively, are observed. In DRB, P02 and P07 are highly contaminated by Pb according to the analyses obtained, not only throughout this study, but also in many investigations carried over the last 10 years. For example, Becouze-Laureure et al. (2016) show that the areas farther from the inlet are more contaminated and that P02 presents highly contaminated sediments. The sediments at P02 and P07 settle slowly, with a mean settling velocity of around 2 mm/s, explained by the two locations being remote from the inlet.

Fig. 8. Comparison of measured and simulated Fe and Pb contents distribution: P01, P02, P04, P07 locations are coloured in blue, orange, black and red, respectively.

4. Discussion

4.1. *Use of Fe as indicator of pollution and for the prediction of contamination distribution*

290 In this study, [Fe] in trapped sediments is strongly related to settling velocity and this relationship is
291 relatively stable from one site to another and from one event to another. In addition, significant
292 correlations between Fe and trace metals are observed (Fig. 7). Other studies have also observed
293 positive correlations between Fe and Cr, Cu, Pb, Ni and Zn in highway stormwater runoff (Kayhanian
294 et al., 2007). Drapeau et al. (2017) revealed a close link among Al, Fe and Si, as well as linear
295 regression between Fe and Cu, Zn, P, S, Si and organic matter in a stormwater infiltration basin.
296 Given the significant correlation between Fe and certain pollutants (here Pb and Cu), the simulated Fe
297 content distribution can then be utilised to understand or to explain the distribution of other particulate
298 pollutants that have affinities with Fe. Besides, iron isotopes have been widely used as tracers to
299 analyse biochemical processes (e.g. metal transport, microbial redox reactions and transformation of
300 organic matter-ferrihydrite coprecipitates), and track sources and other components such as suspended
301 Fe-organic carbon aggregates (Gould et al., 2008; Ingri et al., 2018; Owens et al., 2012; Tishchenko et
302 al., 2015). In DRB, P07 and P02 present the highest maximum values of [Fe] and are also highly
303 contaminated areas given the significant positive correlation between Fe and certain trace metals.
304 Hence, P07 and P02 should be the preferential zones for cleaning.

305 ### 4.2. *Use of settling velocity for stormwater detention basin sediments management*

306 Most studies on the correlation between particle physical and chemical characteristics in stormwater
307 detention basins focus on the relationship between particle size (e.g. Kayhanian, 2012; Tuccillo, 2006)
308 or sediment density (El-Mufleh et al., 2014) and trace metal contents. However, settling velocity
309 should be emphasized given its relationship with other physical characteristics (Loch, 2001). It has
310 been widely applied in urban stormwater management and its importance has been demonstrated

311 (Ciccarello et al., 2012; Yun et al., 2010). Settling velocity is also a key element, when combined with
312 the residence time, for the sizing of stormwater detention basins.

313 The design and management of stormwater detention basins not only need knowledge of
314 hydrodynamic behaviour, but also an understanding of the spatial distribution of highly contaminated
315 sediments. Various modelling approaches (e.g. LDPM) can be used to address the understanding of
316 the velocity field and the spatial distribution of sediment in stormwater detention basins (Adamsson et
317 al., 2003). Given that the particulate fraction of certain metals and PAHs in stormwater from industrial
318 catchments is above 60 % and 80 %, respectively (Becouze-Lareure et al., 2019) and most other
319 pollutants are conveyed in particulate phase (Ashley et al., 2004), the investigation of the correlation
320 between metal contents in sediments and settling velocity may support the coupling between chemical
321 and physical aspects. The final simulation results help to predict pollutant deposition and determine
322 the priority cleaning zones in stormwater detention basins. They may also be used as a support for the
323 design of stormwater detention basins using trapping or removal efficiency as targeted criteria.

324 4.3. *Relationship between sediments' physical and chemical characteristics*

325 The significant correlation between metal contents in sediments and their settling velocity is a key
326 finding of this study. Badin et al. (2008) suggested that organic matter in urban stormwater sediments
327 is related to grain size. Bernardin-Souibgui et al. (2018) found that *Nocardia* counts are positively
328 linked to volatile organic matter. Wiest et al. (2018) revealed that BPA is associated with fine particles.
329 Concerning the physical characteristics, we can analyse particle-size distribution, density and shape
330 related to each fraction of settling velocity to understand their links with chemical characteristics.
331 Given the strong correlation of Fe content with settling velocity, it is interesting to investigate more

thoroughly the oxidation states, isotopes of Fe and the related physical, chemical and biological processes, such as sorption and precipitation (Taylor and Kauhauser, 2011). Besides, other pollutants such as PAHs, organic matter and some pathogenic bacteria can be investigated to see if they are related to metals or settling velocity.

4.4. *Sediment management based on targeted dredging strategy*

The methodology proposed in this article can be applied in any other stormwater detention or retention basin (dry or wet) constructed on a catchment (industrial, urban or periurban) in order to compare and evaluate deriving results against the obtained correlation in this study. This methodology also informs the intervention and treatment of sediments with a focus on the highly contaminated area. In general, the intervention criteria could be determined by comparing the metals contents to the Dutch target and intervention values (DTIV, 2000) and taking into account site specificities. The outcomes of this paper suggest that targeted dredging may be a good alternative for sediment management. In the case of DRB, P02 and P07 are highly contaminated and should be treated promptly. In theory, these contaminated sediments could be stored in places where less recirculation and sediment resuspension phenomenon occur (e.g. the upper-left side of DRB). Indeed, Becouze-Laureure et al. (2018) showed that the ecotoxicity level decreases over time and sediments should thus be left *in situ* before being discharged to a dedicated resource recovery plant or a separation device. Sediments from these most problematic zones could then be separated by means of screening and attrition (Petavy et al., 2009). As the focus is only placed on the problematic areas, less sediments need to be extracted and can be directly treated *in situ*. Such an approach could substantially reduce cost related to sediments transportation, treatment, and reuse.

5. Conclusions

Better understanding of the spatial distribution of trace metal contamination in stormwater detention basins is vital to better manage accumulated sediments and better design such facilities, taking into account the interactions between hydrodynamics and sediment physico-chemical characteristics. Our work investigated the locations of highly contaminated sediments with trace metals in a settling and detention basin by coupling a LDPM with the relationships of sediments' physico-chemical characteristics (correlation between Fe, Cr, Cu, Ni, Pb contents and settling velocity). Based on a large dataset, Fe and Pb contents have a significant correlation with settling velocity, followed by Cu and Cr. The observed significant correlation between Fe content and settling velocity remained stable for all campaigns and sampling sites. An equation describing this correlation is coupled with simulated spatial distribution of sediments to predict Fe content distribution. Obtained results are consistent with *in situ* measurements. Accounting for hydrodynamic behaviour (streamlines exhibiting recirculations, flow shear and turbulence characteristics), particles carrying Fe could then be tracked and used as an indicator to comprehensively identify trace metals contamination areas (e.g. deposition and resuspension zones). This may help to determine the priority cleansing zone in detention basins and better design the stormwater detention basin by taking into consideration all these correlations as well as hydrodynamic parameters in sediments transport equations.

Acknowledgement

This research is supported by OTHU (Observatoire de Terrain en Hydrologie Urbaine), La Métropole du Grand Lyon, ANR CESA CABRRES program (program grant 2011-CESA-012) and CSC Scholarship. In addition, this work was performed within the framework of the EUR H_2O'Lyon

374 (ANR-17-EURE-0018) of Université de Lyon (UdL), within the program "Investissements d'Avenir"
375 operated by the French National Research Agency (ANR). The authors are grateful to David Lebouil
376 for ICP measurement, Dominique Babaud, Serge Naltchayan, Nicolas Walcker and Stéphane Vacherie
377 for technical support. The authors would like also to thank Santiago Sandoval Arenas and Qiufang
378 Zhan for scientific suggestions, Hexiang Yan for providing CFD model data, as well as Prof. Tim
379 Fletcher (the University of Melbourne) and Bonan Cuan for English writing improvements.

380 **References**

381 Adamsson, Å., Stovin, V. R., & Bergdahl, L. (2003). Bed shear stress boundary condition for storage
382 tank sedimentation. Journal of Environmental Engineering, 129(7), 651–658.

383 Akan A.O. (2010). Design aid for water quality detention basins. Journal of Hydrologic Engineering,
384 15(1), 39-48.

385 Ashley, R. M., Bertrand-Krajewski, J. L., Hvitved-Jacobsen, T., & Verbanck, M. (Eds.). (2004). Solids
386 in sewers. IWA Publishing.

387 Badin, A. L., Faure, P., Bedell, J. P., & Delolme, C. (2008). Distribution of organic pollutants and
388 natural organic matter in urban storm water sediments as a function of grain size. Science of the total
389 environment, 403(1-3), 178-187.

390 Barbosa, A. E., Fernandes, J. N., David, L. M. (2012). Key issues for sustainable urban stormwater
391 management. Water Research, 46, 6787-6798.

392 Bardin, J. P., & Barraud, S. (2004). Aide au diagnostic et à la restructuration du bassin de rétention de
393 Chassieu. Rapport INSA-Lyon–URGC Hydrologie Urbaine.

394 Becouze-Lareure, C., Gonzalez-Merchan, C., Sébastian, C., Perrodin, Y., Barraud, S., Lipeme Kouyi,
395 G. (2016). Evolution des caractéristiques physico-chimiques et écotoxicologiques des sédiements
396 accumulés dans un bassin de rétention-décantation : premiers résultats du projet ANR CABRRES.
397 TSM, 4, 43-55.

398 Becouze-Lareure, C., Lipeme Kouyi, G., Gonzalez-Merchan, C., Bazin, C., Sebastian, C., Barraud, S.,
399 & Perrodin, Y. (2018). Spatial and temporal dynamics of sediment ecotoxicity in urban stormwater
400 retention basins: Methodological approach and application to a pilot site close to Lyon in France.
401 Journal of Environmental Science and Health, Part A, 53(13), 1123-1130.

402 Becouze-Lareure, C., Dembélé, A., Coquery, M., Cren-Olivé, C., & Bertrand-Krajewski, J. L. (2019).
403 Assessment of 34 dissolved and particulate organic and metallic micropollutants discharged at the
404 outlet of two contrasted urban catchments. Science of The Total Environment, 651, 1810-1818.

405 Bentzen, T. R., & Larsen, T. (2009). Heavy metal and PAH concentrations in highway runoff deposits
406 fractionated on settling velocities. Journal of Environmental Engineering, 135(11), 1244-1247.

407 Bernardin-Souibgui, C., Barraud, S., Bourgeois, E., Aubin, J. B., Becouze-Lareure, C., Wiest, L., ... &
408 Blaha, D. (2018). Incidence of hydrological, chemical, and physical constraints on bacterial pathogens,
409 Nocardia cells, and fecal indicator bacteria trapped in an urban stormwater detention basin in
410 Chassieu, France. Environmental Science and Pollution Research, 25(25), 24860-24881.

411 Bradl, H. B. (2004). Adsorption of heavy metal ions on soils and soils constituents. Journal of colloid
412 and interface science, 277(1), 1-18.

413 Camponelli, K. M., Lev, S. M., Snodgrass, J. W., Landa, E. R., & Casey, R. E. (2010). Chemical
414 fractionation of Cu and Zn in stormwater, roadway dust and stormwater pond sediments.
415 Environmental pollution, 158(6), 2143-2149.

416 Chapman, P. M., Wang, F., Janssen, C., Persoone, G., Allen, H. E. (1998). Ecotoxicology of Metals in
417 Aquatic Sediments: Binding and Release, Bioavailability, Risk Assessment, and Remediation. Can. J.
418 Fish. Aquat. Sci, 55, 2221–2243.

419 Chebbo, G., & Gromaire, M. C. (2009). ViCAs—An operating protocol to measure the distributions
420 of suspended solid settling velocities within urban drainage samples. Journal of Environmental
421 Engineering, 135(9), 768-775.

422 Ciccarello, A., Bolognesi, A., Maglionico, M., & Artina, S. (2012). The role of settling velocity
423 formulation in the determination of gully pot trapping efficiency: comparison between analytical and
424 experimental data. Water Science and Technology, 65(1), 15-21.

425 Couto, M. F., Peternelli, L. A., & Barbosa, M. H. P. (2013). Classification of the coefficients of
426 variation for sugarcane crops. Ciência rural, 43(6), 957-961.

427 Drapeau C., Delolme C., Chatain V., Gautier M., Blanc D., Benzaazoua M., Lassabatere L. (2017).
428 Spatial and temporal stability of major and trace element leaching in urban stormwater sediments.
429 Open Journal of Soil Science, 7(11), 347-365.

430 DTIV, Dutch target and intervention values. ANNEXES Circular on target values and intervention
431 values for soil remediation, 2000, 51 p.

Dunnett, C. W. A multiple comparisons procedure for comparing several treatments with a control. Journal of the American Statistical Association. 1955, 50 (272): 1096–1121.

El-Mufleh, E., Béchet, B., Basile-Doelsch, I., Geffroy-Rodier, C., Gaudin, A., Ruban, V. (2014). Distribution of PAHs and trace metals in urban stormwater sediments: combination of density fractionation, mineralogy and microanalysis. Environmental Science and Pollution Research, 21, 9764–9776.

Frémion, F., Courtin-Nomade, A., Bordas, F., Lenain, J. F., Jugé, P., Kestens, T., & Mourier, B. (2016). Impact of sediments resuspension on metal solubilization and water quality during recurrent reservoir sluicing management. Science of the Total Environment, 562, 201-215.

Frémion, F., Mourier, B., Courtin-Nomade, A., Lenain, J. F., Annouri, A., Fondanèche, P., ... & Bordas, F. (2017). Key parameters influencing metallic element mobility associated with sediments in a daily-managed reservoir. Science of the Total Environment, 605, 666-676.

Gasperi, J., Sebastian, C., Ruban, V., Delamain, M., Percot, S., Wiest, L., et al. (2014). Micropollutants in urban stormwater: occurrence, concentrations, and atmospheric contributions for a wide range of contaminants in three French catchments. Environmental Science and Pollution Research, 21, 5267-5281.

Gould, W. D., Alpay, S., Smith, C. W., Skaff, M., Lortie, L., & Pawlak, M. (2008). 57Fe as a tracer of bacterially mediated iron mobilization in lake sediments. Geomicrobiology Journal, 25(3-4), 167-180.

Ingri, J., Conrad, S., Lidman, F., Nordblad, F., Engström, E., Rodushkin, I., & Porcelli, D. (2018). Iron isotope pathways in the boreal landscape: Role of the riparian zone. Geochimica et Cosmochimica Acta, 239, 49-60.

Jacopin, C., Bertrand-Krajewski, J. L., & Desbordes, M. (1999). Characterisation and settling of solids in an open, grassed, stormwater sewer network detention basin. Water Science and Technology, 39(2), 135-144.

Jang, Y. C., Jain, P., Tolaymat, T., Dubey, B., Singh, S., & Townsend, T. (2010). Characterization of roadway stormwater system residuals for reuse and disposal options. Science of the total environment, 408(8), 1878-1887.

Kayhanian, M., Suverkropp, C., Ruby, A., & Tsay, K. (2007). Characterization and prediction of highway runoff constituent event mean concentration. Journal of environmental management, 85(2), 279-295.

Kayhanian, M., McKenzie, E. R., Leatherbarrow, J. E., & Young, T. M. (2012). Characteristics of road sediment fractionated particles captured from paved surfaces, surface run-off and detention basins. Science of the total environment, 439, 172-186.

ISO, N. (2000). 13320-1. Particle size analysis: laser diffraction methods.

Konhauser, K. O., Kappler, A., & Roden, E. E. (2011). Iron in microbial metabolisms. Elements, 7(2), 89-93.

Loch, R. J. (2001). Settling velocity- a new approach to assessing soil and sediment properties. Computers and electronics in agriculture, 31, 305-316

470 Maniquiz-Redillas, M. C., Geronimo, F. K. F., Kim, L.-H. (2014). Investigation on the effectiveness
471 of pretreatment in stormwater management technologies. Journal of Environmental science, 26,
472 1824-1830.

473 Marsalek, J., Marsalek, PM. (1997). Characteristics of sediments from a stormwater management
474 pond. Water Science and Technology, 36, 117-122.

475 NF EN 872. (2005). Water quality–Determination of suspended solids–Method by filtration through
476 glass fiber filters.

477 NF EN 16174 (2012). Digestion of aqua regia soluble fractions of elements.

478 NF EN ISO 11885 (1998). Water quality - Determination of selected elements by inductively coupled
479 plasma optical emission spectroscopy (ICP-OES)

480 Owens, J. D., Lyons, T. W., Li, X., Macleod, K. G., Gordon, G., Kuypers, M. M. M., … Severmann, S.
481 (2012). Iron isotope and trace metal records of iron cycling in the proto-North Atlantic during the
482 Cenomanian-Turonian oceanic anoxic event (OAE-2). Paleoceanography, 27(3).
483 doi:10.1029/2012pa002328

484 Persson, J. (2000). The hydraulic performance of ponds of various layouts. Urban Water J. 2(3), 243–
485 250.

486 Petavy, F., Ruban, V., Conil, P., Viau, J. Y., & Auriol, J. C. (2009). Treatment and valorisation of
487 stormwater sediments. Global Nest Journal, 11(2), 189-195.

488 Sébastian, C., Barraud, S., Gonzalez-Merchan, C., Perrodin, Y., & Visiedo, R. (2014a). Stormwater
489 retention basin efficiency regarding micropollutant loads and ecotoxicity. Water Science and
490 Technology, 69(5), 974-981.

491 Sébastian, C., Barraud, S., Ribun, S., Zoropogui, A., Blaha, D., Becouze-Lareure, C., et al. (2014b)
492 Accumulated sediments in a detention basin: chemical and microbial hazard assessment linked to
493 hydrological processes. Environmental Science and Pollution Research, 21, 5367-5378.

494 Sebastian, C., Zhu, J., Vezzaro, L., & Barraud, S. (2014c). Modelling Stormwater Detention Basin
495 Performance in Micropollutant Removal. 13rd International Conference on Urban Drainage, 7-12
496 September 2014, Kuching, Malaysian Borneo. 10 p.

497 Sébastian, C., Becouze-Lareure, C., Kouyi, G. L., & Barraud, S. (2015). Event-based quantification of
498 emerging pollutant removal for an open stormwater retention basin–Loads, efficiency and importance
499 of uncertainties. Water Research, 72, 239-250.

500 Sechet, P. & Le Guennec B. (1999). The role of near wall turbulent structures on sediment transport.
501 Water Research, 33 (17), 3646-365.

502 Shapiro, S. S. & Wilk, M. B. (1965). "An analysis of variance test for normality (complete samples)".
503 Biometrika. 52 (3–4): 591–611. doi:10.1093/biomet/52.3-4.591. JSTOR 2333709. MR 0205384. p.
504 593

505 Taylor, K. G. & Konhauser, K. O. (2011). Iron in Earth surface systems: A major player in chemical
506 and biological processes. Elements, 7(2), 83-88.

507 Tedoldi, D., Chebbo, G., Pierlot, D., Branchu, P., Kovacs, Y., & Gromaire, M. C. (2017). Spatial
508 distribution of heavy metals in the surface soil of source-control stormwater infiltration devices–
509 Inter-site comparison. Science of the total environment, 579, 881-892.

510 Tishchenko, V., Meile, C., Scherer, M. M., Pasakarnis, T. S., & Thompson, A. (2015). Fe2+ catalyzed
511 iron atom exchange and re-crystallization in a tropical soil. Geochimica et Cosmochimica Acta, 148,
512 191-202.

513 Torres, A. & Bertrand-Krajewski, J.-L. (2008). Evaluation of uncertainties in settling velocities of
514 particles in urban stormwater runoff. Water Science and Technology, 57(9), 1389–1396.
515 doi:10.2166/wst.2008.307

516 Torres, A., Hasler, M., Bertrand-Krajewski, J-L. (2007). Spatial heterogeneity and inter-event
517 variability of sediment settling distributions in a stormwater retention tank. Proceedings of 6th
518 NOVATECH conference, Lyon, France.

519 Tuccillo, M. E. (2006). Size fractionation of metals in runoff from residential and highway storm
520 sewers. Science of the Total Environment, 355(1-3), 288-300.

521 Urbonas, B. (1994). Assessment of stormwater BMPs and their technology. Water Science and
522 Technology, 29(1-2), 347-353.

523 Verstraeten, G., and Poesen, J. (2000). Estimating trap efficiency of small reservoirs and ponds:
524 methods and implications for the assessment of sediment yield. Progress in Physical Geography, 24
525 (2), 219-251.

526 Vezzaro, L., Eriksson, E., Ledin, A., & Mikkelsen, P. S. (2010). Dynamic stormwater treatment unit
527 model for micropollutants (STUMP) based on substance inherent properties. Water science and
528 technology, 62(3), 622-629.

529 Whitaker, A., & Duckworth, O. (2018). Cu, Pb, and Zn Sorption to Biogenic Iron (Oxyhydr) Oxides
530 Formed in Circumneutral Environments. Soil Systems, 2(2), 18.

531 Wiest, L., Baudot, R., Lafay, F., Bonjour, E., Becouze-Lareure, C., Aubin, J. B., ... & Vulliet, E.
532 (2018). Priority substances in accumulated sediments in a stormwater detention basin from an
533 industrial area. Environmental Pollution, 243, 1669-1678.

534 Yan, H., Lipeme Kouyi, G., Gonzalez-Merchan, C., Becouze-Lareure, C., Sebastian, C., Barraud, S.,
535 & Bertrand-Krajewski, J. L. (2014). Computational fluid dynamics modelling of flow and particulate
536 contaminants sedimentation in an urban stormwater detention and settling basin. Environmental
537 Science and Pollution Research, 21(8), 5347-5356.

538 Yun, Y., Park, H., Kim, L., & Ko, S. (2010). Size distributions and settling velocities of suspended
539 particles from road and highway. KSCE Journal of Civil Engineering, 14(4), 481-488.

540 Zgheib, S., Moilleron, R., & Chebbo, G. (2008). Screening of priority pollutants in urban stormwater:
541 innovative methodology. Water Pollution IX, 111, 235-244.

542 Zgheib, S., Moilleron, R., Saad, M., Chebbo, G. (2011) Partition of pollution between dissolved and
543 particulate phases: What about emerging substances in urban stormwater catchments? Water Research,
544 45, 913-925.

545 Zgheib S., Moilleron R., Chebbo G. (2012). Priority pollutants in urban stormwater: Part 1 – Case of
546 separate storm sewers. Water Research, 46(20), 6683-6692.

547 Zhang, L. (2009). 3D numerical modeling of hydrodynamic flow, sediment deposition and transport in
548 stormwater ponds and alluvial channels. PhD thesis, Old Dominion University, Virginia, U.S.

549 Zhu X., Claro Barreto A., Lipeme Kouyi G. (2016). Design and performance evaluation of
550 Hydrocyclone and Lamella Settler for Urban Stormwater Sediments. 8th international conference on
551 Sewer Processes and Networks – SPN8, Rotterdam, Netherlands, 31 Aug.-2 Sept.

552 Zhu X., Lipeme Kouyi G., Becouze-Lareure C, Barraud S, Bertrand-Krajewski J.-L. (2017). 3D
553 numerical modelling of resuspension and remobilization of sediments in a stormwater detention basin.
554 Aquaconsoil, Lyon, 26-30 june 2017.

555 Zhu, X., & Lipeme Kouyi, G. (2019). An analysis of LSPIV-based surface velocity measurement
556 techniques for stormwater detention basin management. Water Resources Research, 55(2), 888-903.


a


b

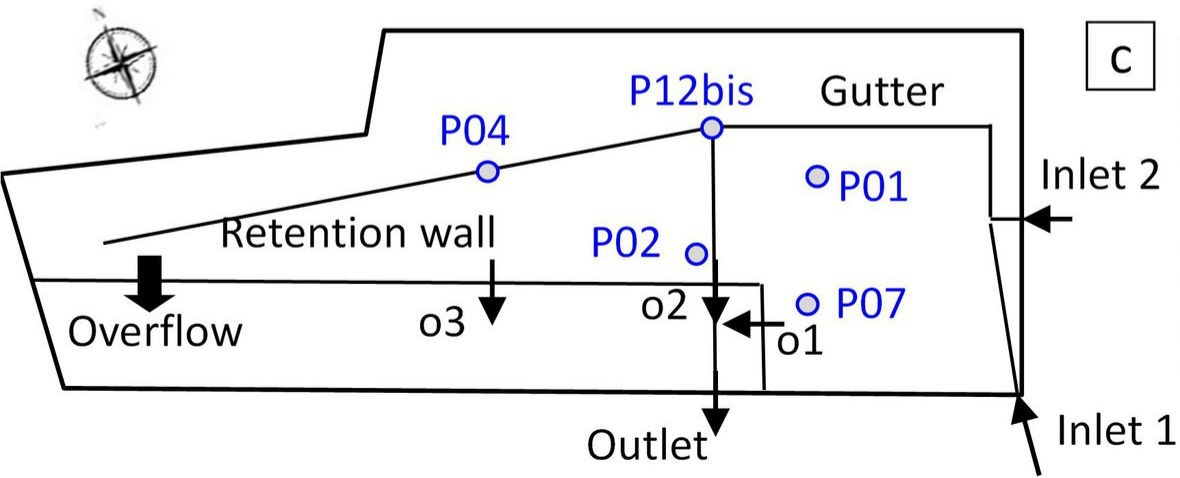
c
P12bis
Gutter
P04
P01
Inlet 2
Retention wall
P02
P07
o3
o2
o1
Overflow
Outlet
Inlet 1


d

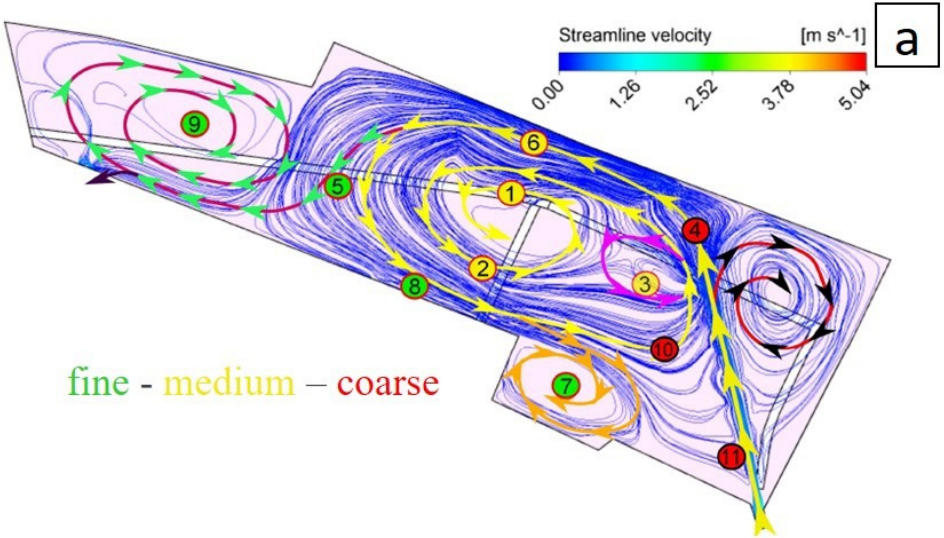
Streamline velocity
[m s^-1]
0.00
1.26
2.52
3.78
5.04
a
9
6
5
1
4
2
3
8
10
7
11
fine - medium – coarse

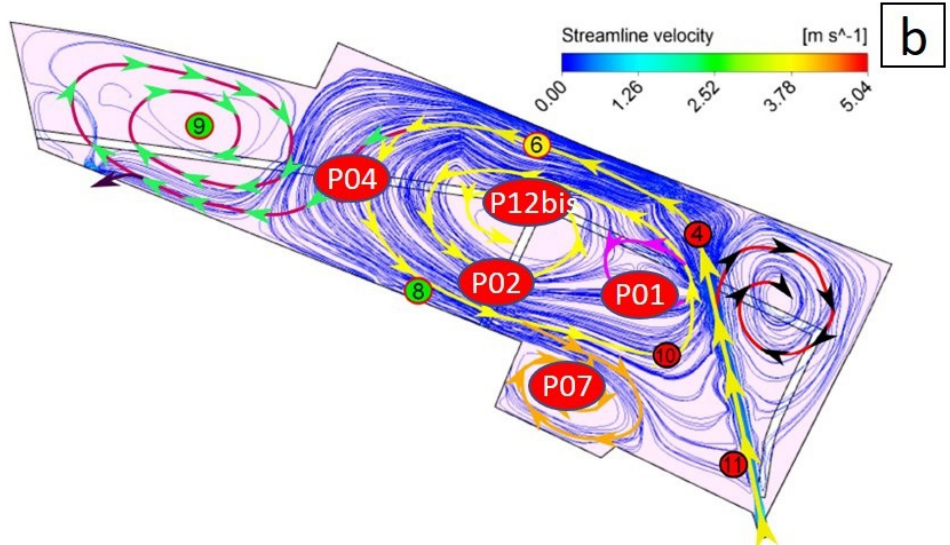
Streamline velocity
[m s^-1]
0.00
1.26
2.52
3.78
5.04
b
9
6
P04
P12bis
4
8
P02
P01
10
P07
11

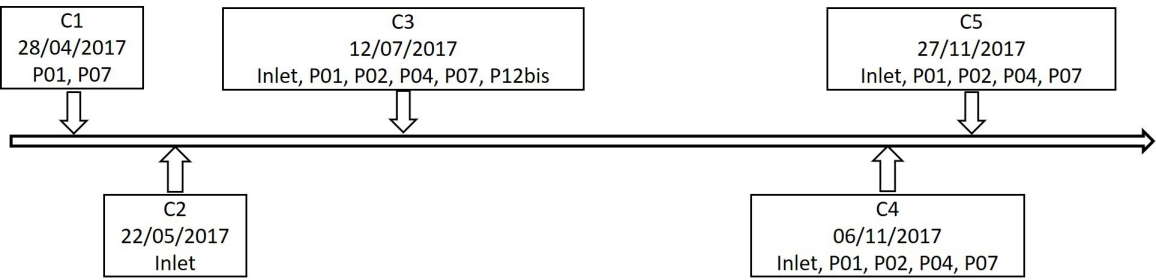
C1
28/04/2017
P01, P07
C3
12/07/2017
Inlet, P01, P02, P04, P07, P12bis
C5
27/11/2017
Inlet, P01, P02, P04, P07
C2
22/05/2017
Inlet
C4
06/11/2017
Inlet, P01, P02, P04, P07

19 Samples from 5 campaigns

Inlet (hydrocyclone system)

Bottom of basin (traps)

Physical and chemical characterization

Data of group I (19 sub-samples):
Particle-size distribution
Settling velocity distribution
Metals contents (Fe, Cr, Cu, Ni, Pb)

Data of group II (190 sub-samples):
10 sub-samples for each of 19 samples,
10 fractions of settling velocities
Metals contents (Fe, Cr, Cu, Ni, Pb) for each fraction of settling velocity

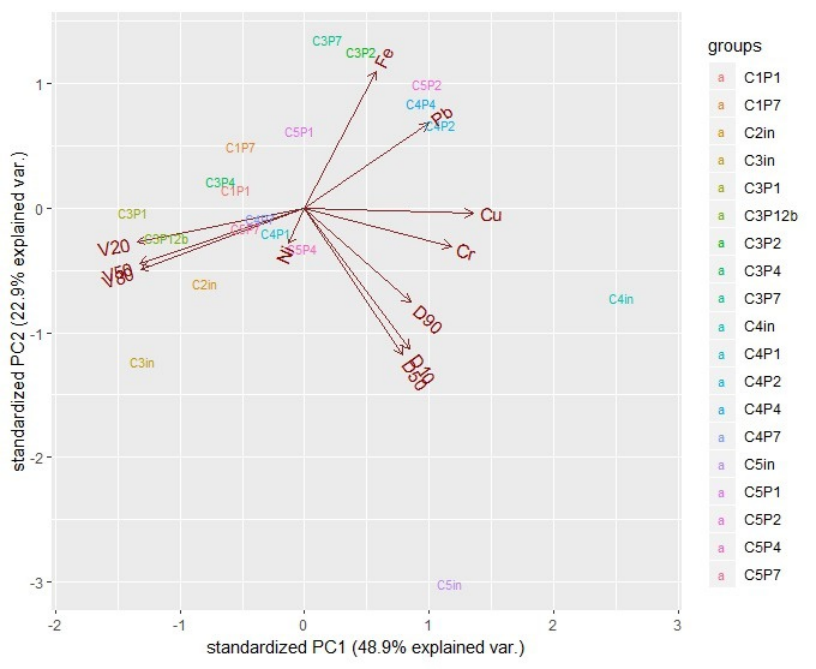
C3P7
C3P2
Fe
C5P2
C4P4
Pb
C4P2
C5P1
C1P7
C3P4
C1P1
C3P1
Cu
V20
C3P12b
C4P1
Ni
C5P4
Cr
V50
V90
C2in
D90
C4in
C3in
D10
D50
C5in
standardized PC2 (22.9% explained var.)
standardized PC1 (48.9% explained var.)
1
0
-1
-2
-3
-2
-1
0
1
2
3
groups
a C1P1
a C1P7
a C2in
a C3in
a C3P1
a C3P12b
a C3P2
a C3P4
a C3P7
a C4in
a C4P1
a C4P2
a C4P4
a C4P7
a C5in
a C5P1
a C5P2
a C5P4
a C5P7

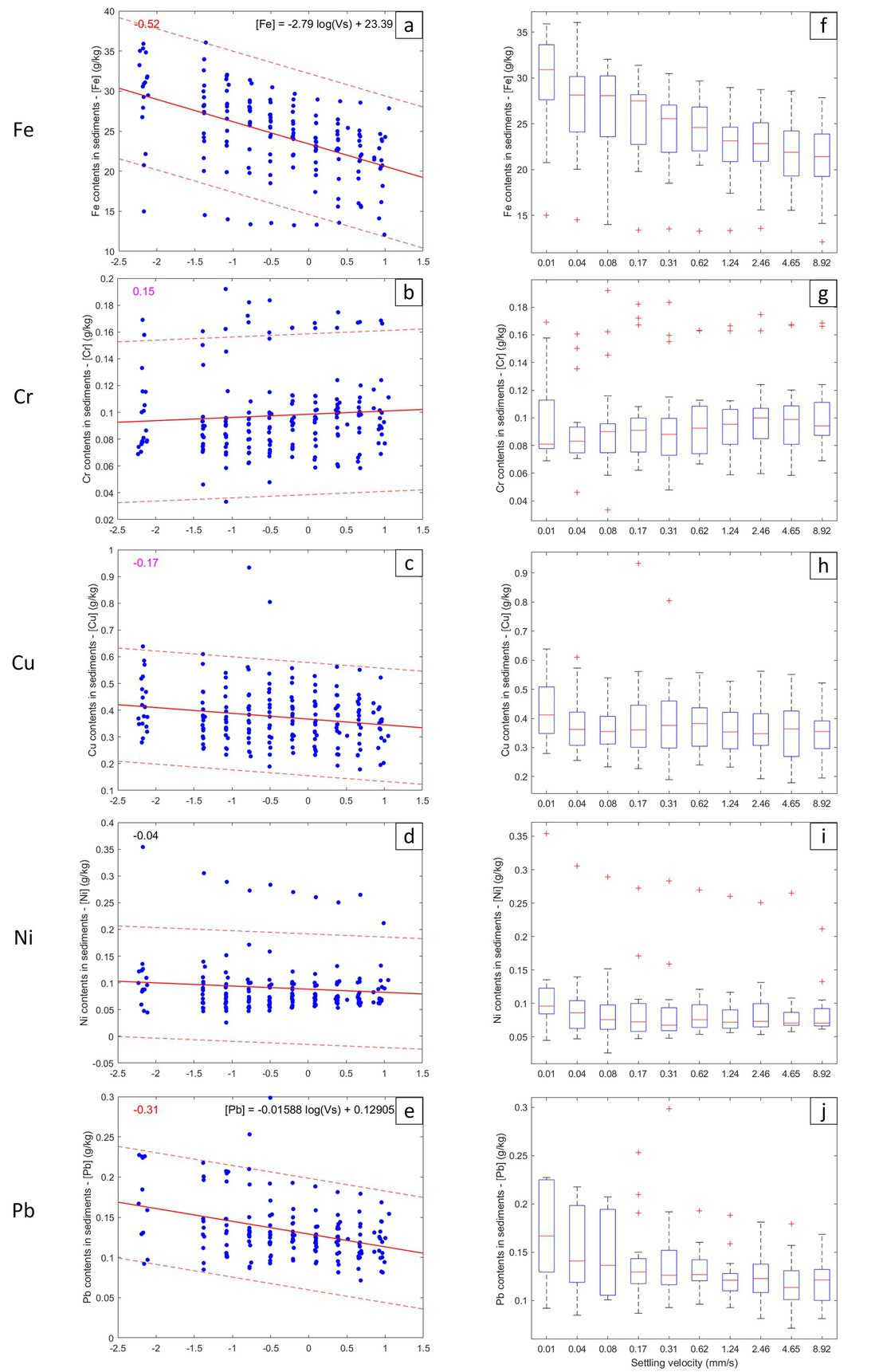

Parameters in (a-e)	Explications
Correlation coefficient	Left-upper side in red (p -value < 0.05/190 according to Eq. 2 with Bonferroni correction) when the correlation is significant; in magenta when p-value < 0.05.
Correlation equation	Right-upper side when the correlation coefficient is significant.
Correlation best fit	Least-squares error minimization, illustrated by red solid lines ———
95% confidence interval	Illustrated by red dashed lines – – –

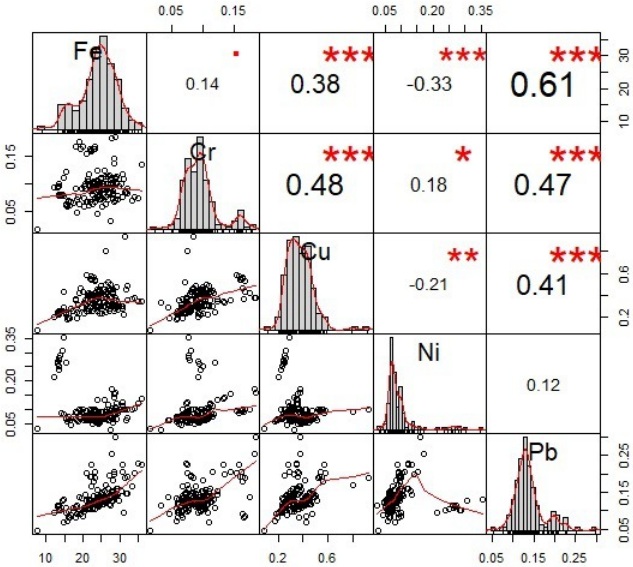
Fe
Cr
Cu
Ni
Pb
0.14
0.38
-0.33
0.61
0.48
0.18
0.47
-0.21
0.41
0.12
***
**
*
.

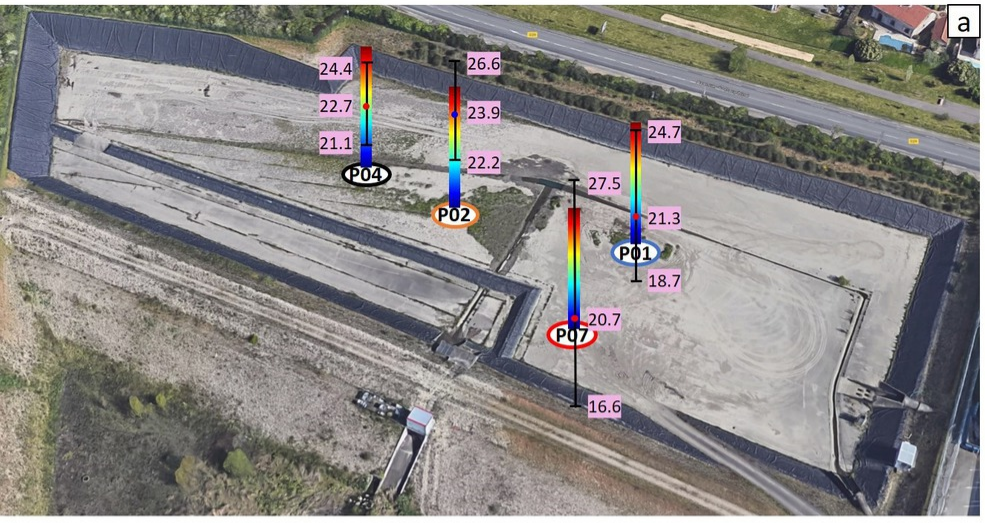

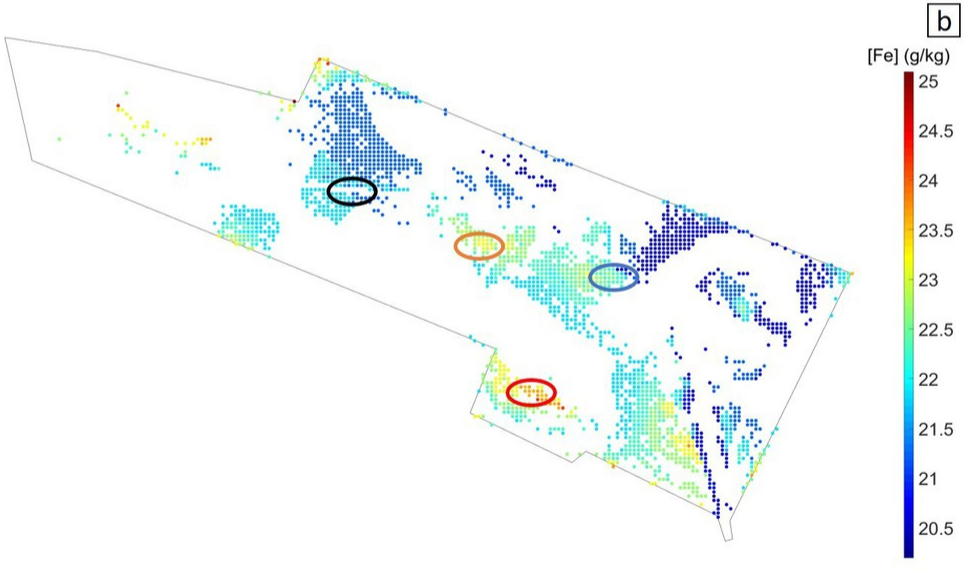

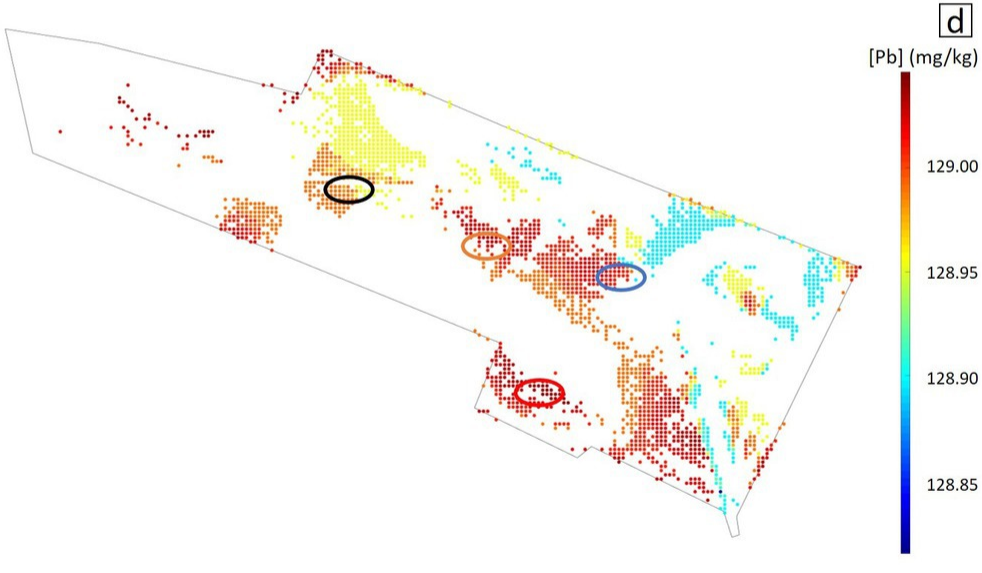

	[Fe] (g/kg DM)	**[Pb] (mg/kg DM)**
Measured [M] at P01, P02, P04 and P07: minimum, averaged and maximum values are plotted, respectively.	a (data of C3-C5 in group I)	c (data of C3-C5 in group I and previous campaign data by Becouze-Laureure et al. (2018))
Simulated median [M] spatial distribution at the bottom of DRB	b: uncertainty of ± 8.8 g/kg (95% confidence interval)	d: uncertainty of ± 69.4 mg/kg (95% confidence interval)

Table 1. Characteristics of DRB

Type of characteristics	Characteristics
Location	Chassieu, France
Type of drainage system	Separated stormwater drainage system
Watershed type	Industrial watershed of 185 ha
Impervious rate of the watershed	75%
Bottom surface area	11 000 m²
Storage capacity	32 000 m^3
Max outlet flow rate limit	0.35 m^3/s (Bardin and Barraud, 2004)
Materials	Bottom in bitumen and banks covered with plastic lining
Compositions	2 inlets (mainly inlet 1 operates, illustrated in Fig. 1b), an outlet, a gutter guiding the flow to 3 orifices during dry periods and an overflow when the water height exceeds the retention wall (presented in Fig.1 c).
Construction and maintenance	Built in 1975, rehabilitated in 2002, cleaned in 2006 and total sediment removal in 2013.

Table 2. Characteristics of the sampled rain events and corresponding hydraulic parameters in DRB

Campaign date	C1	C2	C3	C4	C5
	28/04	22/05	12/07	06/11	27/11
Rainfall characteristics					
Rain Duration (hour:min)	19:22	08:14	03:02	18:26	16:28
Total Depth (mm)	26.5	17.5	10.5	30.9	11.2
Mean Intensity ($mm \cdot h^{-1}$)	1.4	2.1	3.4	1.7	0.7
Max intensity ($mm \cdot h^{-1}$)	6	7.5	58.2	11.7	6.9
ADWP (days)	23	4	8	12	11
DRB hydraulic parameters					
Mean inflow rate (m^3/s)	0.21	0.31	0.24	0.31	0.11
Max inflow rate (m^3/s)	0.76	0.81	1.27	1.08	0.77
Max water level (m)	0.51	0.54	0.39	0.69	0.50

ADWP: antecedent dry weather period

Table 3. Standard and protocols for physical and chemical analyses

Analysis	Method	Standard
Particle-size distribution	Mastersizer 2000 laser diffraction granulometer	NF ISO 13320-1 (2000)
Settling velocity distribution	VICAS protocol (Chebbo et al, 2009)	
Metal content	ICP-OES	NF EN ISO 11885 (1998)

Table 4. Physical and chemical characteristics of trapped sediments

Sample		D50 (µm)	V50 (m/h)	Fe contents (g/kg)	Trace metals contents (mg/kg)			
					Cr	Cu	Ni	Pb
C1	P01	69.2	7.0	nm	74.3	360.1	56.7	98.8
	P07	54.5	6.6	nm	78.3	325.7	54.1	114.3
C2	inlet	55.6	6.7	13.5	96.5	222.0	237.7	99.8
C3	inlet	313.5	11.6	18.2	71.5	242.3	85.2	114.1
	P01	52.9	9.6	20.4	73.5	233.5	74.6	105.7
	P02	37.7	3.4	nm	nm	nm	nm	nm
	P04	45.3	6.9	nm	nm	nm	nm	nm
	P07	45.5	4.1	27.5	93.1	278.8	93.9	137.1
	P12bis	78.3	7.5	15.4	62.7	226.8	70.5	95.8
	mean	95.5	7.2	20.4	75.2	245.4	81.1	113.2
	stdv	107.7	3.2	5.2	12.8	23.1	10.6	17.6
C4	inlet	nm	1.9	21.0	154.3	584.4	93.8	200.6
	P01	144.6	5.9	18.7	76.3	308.7	58.1	96.7
	P02	199.3	2.9	25.6	96.4	457.4	68.7	136.6
	P04	129.4	2.6	24.4	80.5	428.2	61.9	140.7
	P07	79.8	6.7	17.9	89.6	355.3	63.1	111.5
	mean	138.3	4.0	21.5	99.4	426.8	69.1	137.2
	stdv	49.2	2.2	3.4	31.7	105.9	14.3	39.8
C5	inlet	870.5	4.3	14.9	110.4	429.0	80.4	69.7

	P01	78.5	6.0	24.7	94.9	349.2	65.7	115.7
	P02	100.2	2.1	22.2	89.1	378.3	72.7	167.2
	P04	433.3	5.4	21.1	65.8	258.1	59.2	112.3
	P07	109.8	5.7	16.6	66.3	275.0	42.7	88.9
	mean	318.5	4.7	19.9	85.3	337.9	64.1	110.8
	stdv	341.6	1.6	4.0	19.2	71.4	14.4	36.6
inlet	mean	413.2	6.1	16.9	108.2	369.4	124.3	121.1
	stdv	416.5	4.2	3.4	34.7	170.9	75.8	56.2
P01	mean	86.3	7.1	21.3	79.7	312.9	63.8	104.2
	stdv	40.3	1.7	3.1	10.1	57.3	8.2	8.6
P02	mean	112.4	2.8	23.9	92.8	417.8	70.7	151.9
	stdv	81.5	0.6	2.4	5.1	55.9	2.9	21.6
P04	mean	202.7	5.0	22.7	73.2	343.2	60.5	126.5
	stdv	204.1	2.2	2.4	10.4	120.3	1.9	20.1
P07	mean	72.4	5.8	20.7	81.8	308.7	63.5	113.0
	stdv	28.9	1.2	6.0	12.1	38.7	22.0	19.7

D50: median particle size, V50: median settling velocity, nm: not measured, stdv: standard deviation

Sampling

Characterization

Vs = H/t
[M]

Correlation

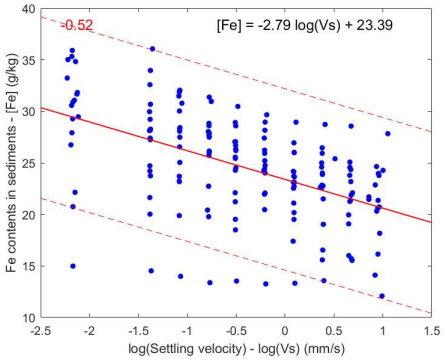

Contamination distribution